ORGANOMETALLICS

ARTICLE

pubs.acs.org/Organometallics

Chiral Silver and Gold Rings: Synthesis and Structural, Spectroscopic, and Photophysical Properties of Ag and Au Metallamacrocycles of Bridging NHC Ligands

Cristina Carcedo, James C. Knight, Simon J. A. Pope, Ian A. Fallis,* and Athanasia Dervisi*

School of Chemistry, Cardiff University, Main Building, Park Place, Cardiff CF10 3AT, U.K.

Supporting Information

ABSTRACT: The synthesis and silver(I) and gold(I) coordination chemistry of a new chiral, bidentate N-heterocyclic carbene (NHC) dehydrohexitol derivative (**3**) are reported. The imidazolium salt $[H_2\mathbf{3}][PF_6]_2$ reacts with Ag_2O and Au(tht)Cl (tht = tetrahydrothiophene) precursors to form the isostructural 18-membered metallamacrocyclic dimers $[Ag_2(\mu\text{-}\mathbf{3})_2][PF_6]_2$ and $[Au_2(\mu\text{-}\mathbf{3})_2][PF_6]_2$ and the monocarbene complex $[(AuCl)_2(\mu\text{-}\mathbf{3})]$. Single-crystal X-ray structures have been determined for the bis-imidazolium precursor $[H_2\mathbf{3}][PF_6]_2$ and corresponding Ag(I) and Au(I) complexes of ligand **3**. Comparison between the X-ray-derived structures and solution-phase NMR data for $[Ag_2(\mu\text{-}\mathbf{3})_2][PF_6]_2$ and $[Au_2(\mu\text{-}\mathbf{3})_2][PF_6]_2$ demonstrate that the complexes adopt a conformation in solution different from that found in the solid state, implying a conformational flexibility of the metallamacrocycle in solution. Both $[(AuCl)_2(\mu\text{-}\mathbf{3})]$ and $[Au_2(\mu\text{-}\mathbf{3})_2][PF_6]_2$ are emissive in the solid state at ca. 380 nm (λ_{ex} = 295 nm). Time-resolved luminescence measurements indicate different excited-state lifetimes for the two species, with $[(AuCl)_2(\mu\text{-}\mathbf{3})]$ measured at 35 ns and $[Au_2(\mu\text{-}\mathbf{3})_2][PF_6]_2$ at 379 ns. The chiroptical properties of the silver and gold NHC complexes have been studied by circular dichroism (CD).

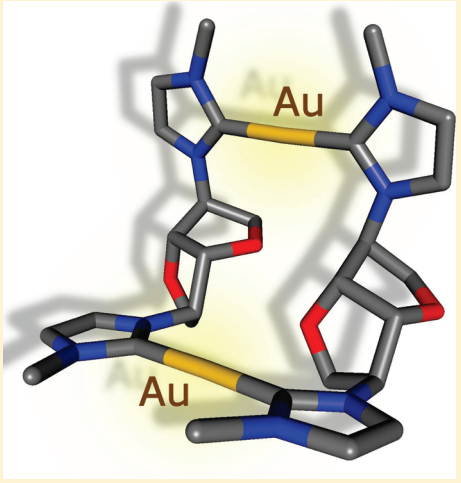

INTRODUCTION

Closed-shell silver and gold complexes have attracted much interest due to their unusual bonding and photophysical properties.[1] More recently, Ag(I) and Au(I) N-heterocyclic carbene (NHC) ligand complexes[2] have appeared in the literature with a large array of structural motifs ranging from two-coordinate linear molecules[3] to complex helical structures,[4] polymers,[5] rings,[6] cages,[7] and clusters.[8] Many of these have potential uses in high-end materials applications such as luminescent chemosensors[9] and optoelectronic on−off switches.[10] Ag(I)− and Au(I)−NHC complexes have also found many medicinal applications, the former mainly due to their activity as antimicrobials[11] and the latter as chemotherapeutic agents.[12] In addition, silver(I) carbenes are extensively used as efficient ligand transfer agents for the majority of imidazolium and other azolium salts, forming part of a convenient and sometimes essential route for the synthesis of metal carbene complexes.[13]

Of the many structurally characterized silver(I) and gold(I) NHC complexes, there are relatively few examples with a metallamacrocyclic structure and, to the best of our knowledge, none with a chiral bridging framework.[14] Previously, we have exploited the chiral framework of the precursor isomannide (**1**; Scheme 1) to prepare a chelating bis-diphenylphosphine with endo stereochemistry which formed stable chelating complexes with transition metals, despite the rigid sterically demanding fused-ring backbone.[15] Isomannide is an inexpensive starch-industry by-product obtained from the dehydration of mannitol. Our interest in the use of this auxiliary in the development of multifunctional ligands stems from the steric control exerted from its hinged backbone. We have now extended the uses of isomannide in ligand design by preparing the bis-imidazole carbene precursor $[H_2\mathbf{3}][PF_6]_2$ (Scheme 1) with 2,5-exo stereochemistry (the endo and exo prefixes here refer to substitution with respect to the bent V-shaped core of the fused dehydrohexitol ring). In this paper we report the synthesis of the isomannide-derived bis-methylimidazolium NHC precursor salt $[H_2\mathbf{3}][PF_6]_2$ and its deprotonation and in situ coordination with group 11 metals to form chiral-NHC silver and gold metallamacrocyclic complexes.

RESULTS AND DISCUSSION

Synthesis of $[H_2\mathbf{3}][PF_6]_2$. The bis-methylimidazolium iodide salt $[H_2\mathbf{3}][PF_6]_2$ was prepared from the commercially available diol isomannide in three steps (Scheme 1). The ditosylate **2** was obtained from the reaction of isomannide with tosyl chloride in cold pyridine in respectable yields. Heating the ditosylate **2** with an excess of methylimidazole at 140 °C afforded

Received: February 11, 2011
Published: April 06, 2011

dx.doi.org/10.1021/om200125w | *Organometallics* 2011, 30, 2553–2562

Scheme 1[a]

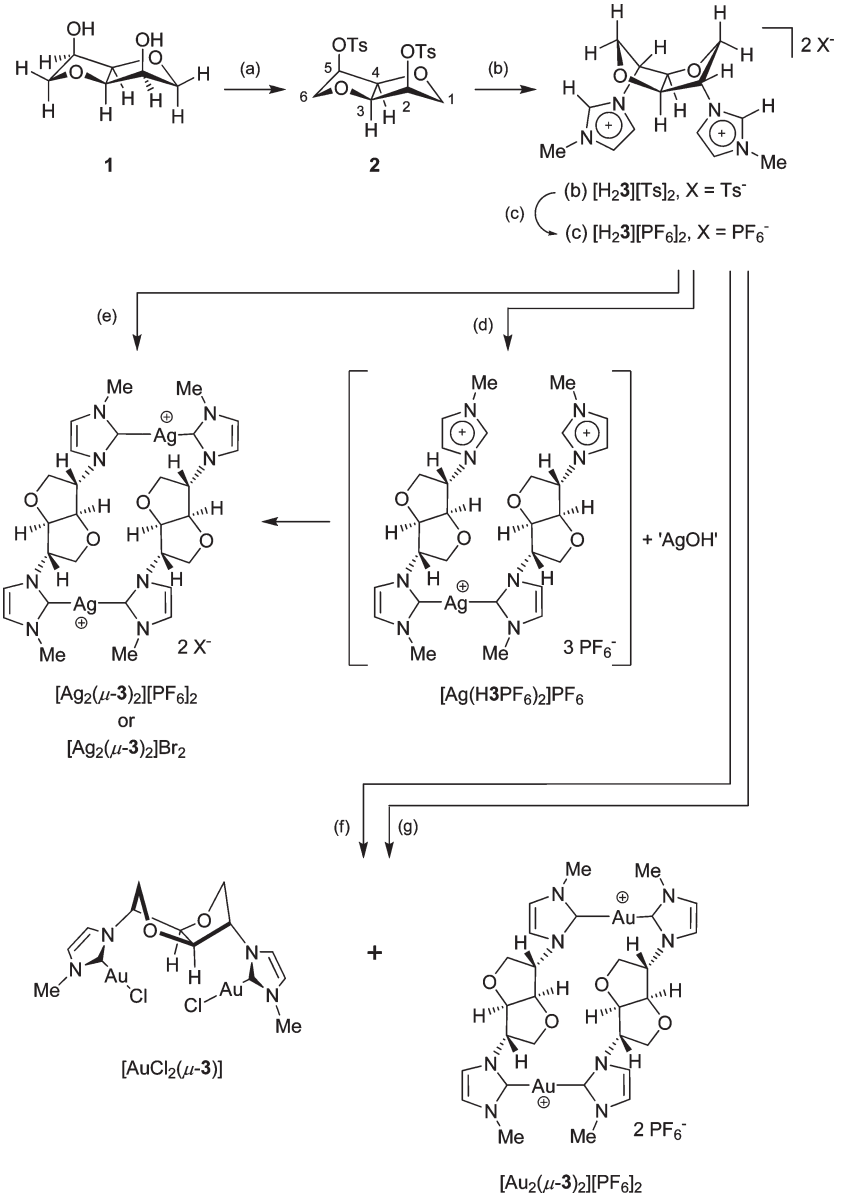

[a] Reagents, conditions, and yields: (a) TsCl, pyridine, 4 °C, 75%; (b) *N*-methylimidazole, 140 °C, neat, 99%; (c) excess NH_4PF_6, H_2O, 64%; (d) Ag_2O, NaBr, CH_2Cl_2, room temperature, 2 days, 85%; (e) for $[Ag_2(\mu\text{-}3)_2]Br_2$, excess Ag_2O, $[N(C_3H_7)_4]Br$; (f) [AuCl(tht)], NaOAc, 70−110 °C, DMF, 30 min, 31% $[Au(\mu\text{-}3)]_2[PF_6]_2$ and 62% $[(AuCl)_2(\mu\text{-}3)]$; (g) [AuCl(tht)], NaOAc, 70−110 °C, DMA, 2 h, 4% $[Au(\mu\text{-}3)]_2[PF_6]_2$ and 55% $[(AuCl)_2(\mu\text{-}3)]$.

the corresponding ditosylate salt $[H_23][Ts]_2$ as a thick brown oil in quantitative yields. This reaction proceeds cleanly to furnish the expected S_N2 inversion product with no isomerization byproduct observed in this case. Counterion metathesis with ammonium hexafluorophosphate in water furnished $[H_23][PF_6]_2$ as a crystalline white solid in 64% yield. The imidazolium salts $[H_23][Ts]_2$ and $[H_23][PF_6]_2$ have the expected exo stereochemistry at the 2- and 5-positions of the bicyclic ring, the same as in the parent hexitol, iditol. The dicationic salts are readily soluble in polar organic solvents such as acetonitrile and DMSO. The ditosylate salt is also freely soluble in water, with the PF_6 analogue dissolving only sparingly in water at room temperature.

^{1}H NMR data for $3\cdot(HPF_6)_2$ are shown in Table 1, and the numbering scheme adopted for the core bicyclic protons is shown for compound **2** in Scheme 1. Assignments for the endo and exo methylene protons ($H^{1/6}$) were made on the basis of their vicinal coupling values with the methine protons $H^{2/5}$. The signal for the bridgehead protons ($H^{3/4}$) appears as a singlet as a result of the close to 90° angle formed with the vicinal $H^{2/5}$ protons, a common feature for the exo-substituted iditol derivatives. The azolium proton has a relatively high chemical shift at δ 8.47 ppm associated with H bonding to the O atoms of the dioxabicyclo unit (vide infra). Worth noting from the ^{13}C NMR data (Table 1) is the large downfield shift for the $C^{3/4}$ atoms of $[H_23][PF_6]_2$ in comparison with those of the ditosylate derivative **2**. Such large downfield changes from endo to exo dehydrohexitol derivatives have been attributed to steric compression effects (field effect) of the more crowded endo derivatives.[16]

dx.doi.org/10.1021/om200125w |*Organometallics* 2011, 30, 2553–2562

Table 1. Selected ^{1}H and ^{13}C NMR Data for the Compounds of 3[a]

compd	*endo*-H$^{1/6}$ (J_{HH})	*exo*-H$^{1/6}$ (J_{HH})	H$^{2/5}$ (J_{HH})	H$^{3/4}$ (J_{HH})	C$^{1/6}$	C$^{2/5}$	C$^{3/4}$
2[b]	3.65 (9.6, 7.7)	3.83 (9.6, 6.8)	4.78 (m)	4.40 (m)	71.6	79.9	81.6
$[H_2\mathbf{3}][PF_6]_2$	4.34 (11.4, 4.9)	4.27 (11.4, 2.4)	5.13 (4.9, 2.4)	5.02 (~0)	72.86	66.21	88.15
$[Ag_2(\mu\text{-}\mathbf{3})_2][PF_6]_2$	4.23 (11.0, 5.1)	4.43 (11.0, 0.7)	5.20 (5.1, 0.7)	4.74 (~0)	73.16	66.51	88.59
$[Au_2(\mu\text{-}\mathbf{3})_2][PF_6]_2$	4.44 (10.8, 6.0)	4.55 (10.8, 3.3)	5.18 (6.0, 3.3)	5.07 (br, ~0)	71.20	65.98	87.82
$[(AuCl)_2(\mu\text{-}\mathbf{3})]$	4.35 (10.8, 5.4)	4.23 (10.8, 2.7)	5.36 (5.4, 2.7)	4.93 (br, ~0)	71.46	66.14	87.48

[a] In CD_3CN unless otherwise noted. Chemical shifts are given in ppm and *J* values in Hz. [b] In $CDCl_3$.

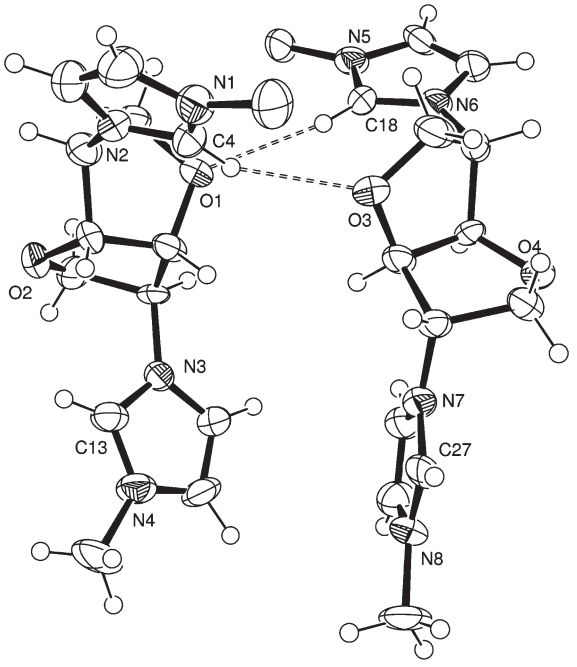

Figure 1. Displacement ellipsoid plots at 30% probability of the imidazolium cation $[H_2\mathbf{3}][PF_6]_2$. Two cations from the unit cell are shown, with the PF_6 anions and selected protons omitted for clarity. Selected bond lengths (Å) and angles (deg): N−C_{NHC}(av) = 1.339(10), O(1)···H(18) = 2.391, O(3)···H(4) = 2.396; O(1)···H(18)−C(18) = 145.8, O(3)···H(4)−C(4) = 146.7.

Single crystals of $[H_2\mathbf{3}][PF_6]_2$ suitable for X-ray studies were grown from a water solution of the salt. Several hydrogen-bonding interactions between the dioxolane and imidazolium protons with the ether oxygen and PF_6^- anion are observed in the solid state. Figure 1 shows two of the four $[H_2\mathbf{3}][PF_6]_2$ molecules in the unit cell linked via hydrogen-bonding interactions between the imidazolium proton and the ether function of the neighboring cation. The molecular packing of the imidazolium salt, supported by intermolecular hydrogen bonding, is shown in Figure 2. This alternating packing arrangement produces wave-like channels running parallel to the *a* axis.

Complexes of 3. The bis-NHC ligand **3** was anticipated to form bridging, linear coordination polymers[17] or cyclic arrays with the metals Ag(I) and Au(I), bearing either one or two NHC donors per metal. The bis-imidazolium salt $[H_2\mathbf{3}][PF_6]_2$ was reacted directly with Ag(I) and Au(I) precursors to form the corresponding NHC complexes without the need to preform or isolate the carbene ligand **3**.

The NHC precursor $[H_2\mathbf{3}][PF_6]_2$ was reacted with freshly prepared silver oxide in dichloromethane or DMSO to produce

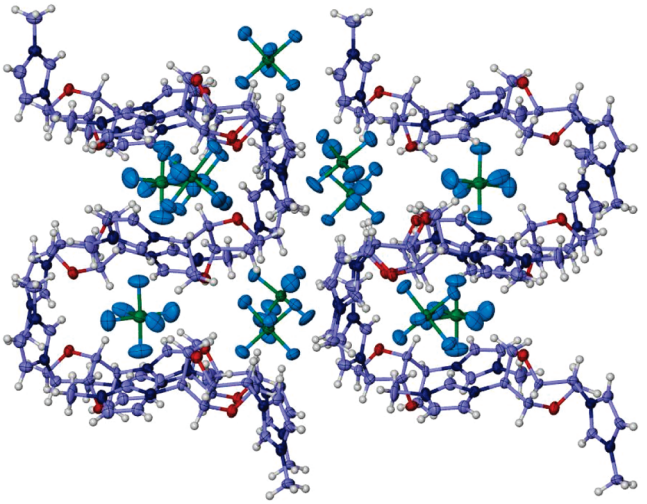

Figure 2. View of the molecular packing for $[H_2\mathbf{3}][PF_6]_2$ along the *a* axis.

the silver-bridged macrocycle $[Ag_2(\mu\text{-}\mathbf{3})_2][PF_6]_2$. This was the only silver complex observed even when an excess of Ag_2O was used in order to gain access to Ag−monocarbene complexes, e.g. **4**. Further attempts to produce a monomeric complex using excess Ag_2O and tetrapropylammonium bromide failed, giving only the dimeric complex $[Ag_2(\mu\text{-}\mathbf{3})_2]X_2$, with a mixture of Br^- and PF_6^- counterions. ^{1}H NMR spectra (CD_3CN) taken during the course of the reaction revealed the formation of the intermediate biscarbene-imidazolium complex $[Ag(H\mathbf{3}PF_6)_2][PF_6]$ (see Scheme 1).

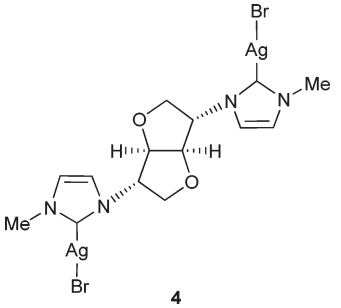

4

The isostructural gold complex $[Au_2(\mu\text{-}\mathbf{3})_2][PF_6]_2$ was isolated from the 1:1 reaction of Au(tht)Cl (tht = tetrahydrothiophene) and $[H_2\mathbf{3}][PF_6]_2$ in hot DMF in the presence of sodium acetate, as a weak base. In this case, however, the linear gold complex $[(AuCl)_2(\mu\text{-}\mathbf{3})]$ was also formed in an approximate 2:1 molar ratio (as determined by ^{1}H NMR) with the digold macrocycle. It is logical to suggest that the Au(tht)Cl precursor favors formation of

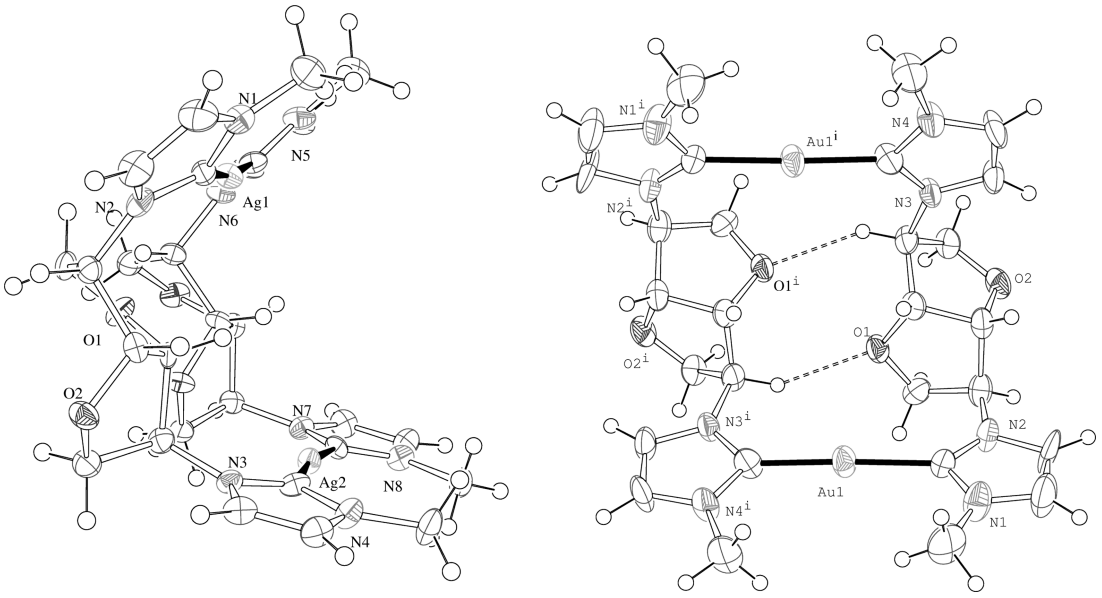

Figure 3. ORTEP ellipsoid plots at the 30% probability level of the cations $[Ag_2(\mu\text{-}\mathbf{3})_2]^{2+}$ (left; side view of the Ag coordination axes) and $[Au_2(\mu\text{-}\mathbf{3})_2]^{2+}$ (right; front view of the Au coordination axes). Selected bond lengths (Å) and angles (deg): $[Ag_2(\mu\text{-}\mathbf{3})_2][PF_6]_2$, Ag(1)−C(2) = 2.107(6), Ag(1)−C(16) = 2.103(6), Ag(2)−C(14) = 2.096(6), Ag(2)−C(28) = 2.123(6), C(16)−Ag(1)−C(2) = 171.7(3), C(14)−Ag(2)−C(28) = 171.7(3); $[Au_2(\mu\text{-}\mathbf{3})_2][PF_6]_2$, C(1)−Au(1) = 2.046(10), C(11)−Au(1)^{i} = 1.983(10), C(11)^{i}−Au(1)−C(1) = 177.6(4). Hydrogen-bonding interactions are indicated by dashed lines.

the Au(NHC)Cl complex. A change in reaction solvent to dimethylacetamide (DMA) shifted the product distribution of this reaction to favor $[(AuCl)_2(\mu\text{-}\mathbf{3})]$ as the major product (55% yield), with only a minor $[Au_2(\mu\text{-}\mathbf{3})_2][PF_6]_2$ component (4% yield) being observed. The 2:1 reaction of Au(tht)Cl and $[H_2\mathbf{3}][PF_6]_2$ in hot DMA afforded the monocarbene complex $[(AuCl)_2(\mu\text{-}\mathbf{3})]$, but the product was contaminated with unreacted $[H_2\mathbf{3}][PF_6]_2$ and ill-defined intermediate Au-NHC species. Alternatively, the gold macrocycle can be obtained via transmetalation of the silver complex $[Ag_2(\mu\text{-}\mathbf{3})_2][PF_6]_2$. However, this approach afforded the product in reduced yield. All complexes were soluble in polar solvents such as acetonitrile, DMF, and DMSO. $[(AuCl)_2(\mu\text{-}\mathbf{3})]$ was also soluble in chlorinated solvents such as CH_3Cl and CH_2Cl_2.

The silver(I)−carbene complexes have been extensively used as carbene transfer agents to other transition metals, most commonly palladium and to a lesser extent rhodium and iridium.[13] Several attempts were made, employing different synthetic routes for the transmetalation of $[Ag_2(\mu\text{-}\mathbf{3})_2][PF_6]_2$ with various Pd(II) salts. Reactions, however, led to partial protonolysis to the parent imidazolium salt $[H_2\mathbf{3}][PF_6]_2$, and any well-defined palladium−NHC complexes formed proved difficult to isolate and characterize further.

Solid-State Structures. The solid-state structures for both the silver and gold metallacycle complexes were determined, confirming their ring structure. Both compounds are cationic comprised of a bimetallic core, $[M_2(\mu\text{-NHC})_2]^{2+}$, linked by a pair of bridging carbene ligands. The two isostructural dimers adopt an "open" C_2-symmetric conformation placing the C_{NHC}−M−C_{NHC} axes parallel to each other and the carbene rings on the same metal atom in a coplanar orientation (Figure 3) with the gold complex bearing a true C_2 crystallographic axis, rendering the two Au fragments equivalent. The dioxolane linker imposes a cleft between the constituent planes of the cations with a fold angle between the two $M(NHC)_2$ planes at 82.4(7)° for $[Au_2(\mu\text{-}\mathbf{3})_2]^{2+}$ and 74.6(4)° for the silver cation. Due to this large opening no argentophilic or aurophilic interactions are observed between the two metal centers for either $[Ag_2(\mu\text{-}\mathbf{3})_2]^{2+}$ or $[Au_2(\mu\text{-}\mathbf{3})_2]^{2+}$ cations, with intermetallic distances of 5.558 and 6.293 Å, respectively.[18] In the silver dimer the two metal atoms bend toward each other with a 171.7(3)° C−Ag−C angle, whereas in the gold analogue the C−Au−C angle is closer to linear at 177.6(5)°.

The two carbenoid rings of the $M(NHC)_2$ fragments adopt nearly coplanar orientations. The interplanar "tilt" angle between the adjacent heterocycle planes in the $[Au_2(\mu\text{-}\mathbf{3})_2]^{2+}$ cation is 8.7(9)°, with the gold atom deviating from the associated planes by relatively small amounts, 0.0412(4) and 0.0917(5) Å, indicating essential coplanarity. In the case of the silver dimer, though, bending of the N(1,2) imidazole ring relative to its Ag−C_{NHC} bond is observed by ca. 12°, associated with the Ag(1) atom divergence by 0.4091(4) Å from the N(1,2) ring plane. However, small deviations are observed for the silver atoms from the remaining carbenoid planes by 0.0710(4), 0.1711(4), and 0.1351(4) Å, respectively, with the interplanar tilt angle for the N(3,4) and N(7,8) containing rings at 4.0(5)°.

As shown in Figure 3, small differences are observed in the Ag−C(2,14,16,28) distances (r_{av} = 2.107(6) Å) for $[Ag_2(\mu\text{-}\mathbf{3})_2][PF_6)]_2$; this average is somewhat longer when compared to those for other bis-imidazolyl Ag complexes but probably reflects the steric restrictions of a macrometallacyclic structure.[2d,19] The Au−C(1,11) bond distances at 2.042(11) and 1.985(11) Å, as expected, are significantly shorter than those of the Ag isomer, due to the smaller covalent radii of Au,[20] but are comparable to the values for other bridging $Au(NHC)_2^+$ complexes.[14,21]

Both structures in the solid state form H bonds with the PF_6 anions and, more interestingly, H bonds between the "endo" oxygen atoms (facing into the metallacycle ring) with the methine protons ($H^{2/5}$) opposite them (Figure 3, Table 2). Values for the H bonds are 2.57/2.72 and 2.31 Å for the silver and gold complexes, respectively.

dx.doi.org/10.1021/om200125w |*Organometallics* 2011, 30, 2553–2562

Table 2. H Bonding between Endo Oxygen Atoms in $[Au(\mu\text{-}3)(PF_6)]_2$ and $[Ag(\mu\text{-}3)(PF_6)]_2$[a]

compd	D−H···A	d(D−H), Å	d(H···A), Å	d(D···A), Å	∠(DHA), deg
$[Au_2(\mu\text{-}3)_2][PF_6)]_2$	C9−H9···O1_#1	1.00	2.31	3.170(14)	144.1
$[Ag_2(\mu\text{-}3)_2][PF_6)]_2$	C19−H19···O1	1.00	2.57	3.439(8)	145.1
	C10−H10···O4	1.00	2.72	3.560(8)	142.3

[a] Symmetry transformation used to generate equivalent atoms: (#1) $^1/_2 - x, y, 1 - z$.

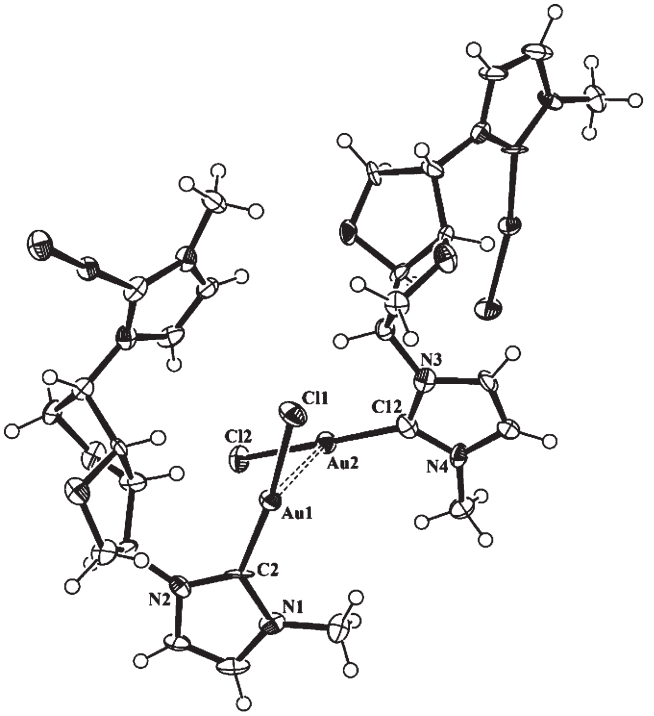

Figure 4. ORTEP ellipsoid plot at the 30% probability level of $[(AuCl)_2(\mu\text{-}3)]$. Selected bond lengths (Å) and angles (deg): C(2)−Au(1) = 1.969(10), C(12)−Au(2) = 1.974(13), Au(1)−Cl(1) = 2.278(3), Au(2)−Cl(2) = 2.285(3), Au(1)···Au(2) = 3.2948(7); Cl(1)−Au(1)−C(2) = 170.8(4), Cl(2)−Au(2)−C(12) = 173.4(4), C(2)−Au(1)−Au(2) = 91.7(3), Cl(1)−Au(1)−Au(2) = 95.85(10), C(12)−Au(2)−Cl(2) = 173.4(4), Cl(2)−Au(2)−Au(1) = 93.9(4), Cl(2)−Au(2)−Au(1) = 92.54(9), Cl(1)−Au(1)−Au(2)−C(12) = 55.4(4), Cl(2)−Au(2)−Au(1)−C(2) = 49.0(4).

An ORTEP representation of the solid-state structure of the gold chloride complex $[(AuCl)_2(\mu\text{-}3)]$ is shown in Figure 4. In the solid state, $[(AuCl)_2(\mu\text{-}3)]$ molecules are linked by closed shell $d^{10}-d^{10}$ aurophilic interactions forming infinite chains, with the two interacting gold units arranged in a staggered fashion. The Au(1)···Au(2) separation between adjacent gold centers is 3.2948(7) Å, close to the sum of their van der Waals radii (3.32 Å).[22] Although shorter Au···Au distances have been previously reported for AuCl(NHC) complexes (ca. 3.16 Å),[3d,9] the observed Au(1)···Au(2) separation for $[(AuCl)_2(\mu\text{-}3)]$ is well within the limits for aurophilic interactions.[1a]

Solution Studies. The silver and gold metallacycle complexes of **3** preserve their dimeric structure in solution, as confirmed by NMR, conductivity, and MS measurements. Electrospray mass spectrometry shows maximum mass peaks at m/z 907 and 1087 for the silver and gold complexes, respectively, corresponding to loss of one of the PF_6 anions from the parent molecule, $[M(\mu\text{-}3)]_2[PF_6]_2$.

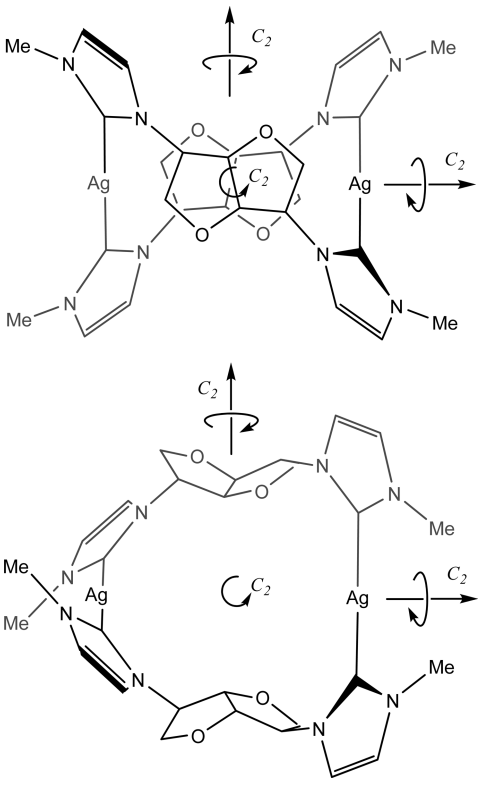

Figure 5. Line drawing representation of the side and top views of the metallamacrocyclic ring of $[Ag_2(\mu\text{-}3)_2][PF_6)]_2$ in a D_2-symmetric conformation.

Data from the ^1H and ^{13}C NMR spectra of the silver and gold complexes of **3** are given in Table 1. The ^1H NMR spectra of $[Ag_2(\mu\text{-}3)_2][PF_6]_2$ and $[Au_2(\mu\text{-}3)_2][PF_6]_2$ show four distinct resonances for the dioxolane core protons, suggesting a conformation of higher symmetry in solution than the C_2 symmetry observed in the solid state. The "open" chain conformation (eq 1) of the crystal structures shown in Figure 3 renders all eight protons of the dioxolane unit nonequivalent, whereas in the higher D_2 symmetry of the "folded" chain conformations (Figure 5) the respective protons $H^{1/6}$(endo), $H^{1/6}$(exo), $H^{2/5}$, and $H^{3/4}$ are equivalent (numbering shown in Scheme 1, structure **2**).

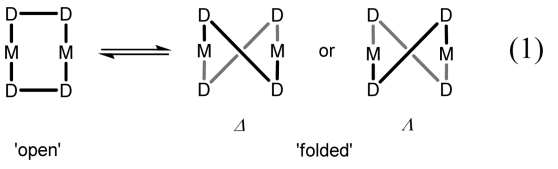

(1)

The D_2-symmetric conformation shown in Figure 5 is sterically less demanding than the C_2 conformation adopted in the

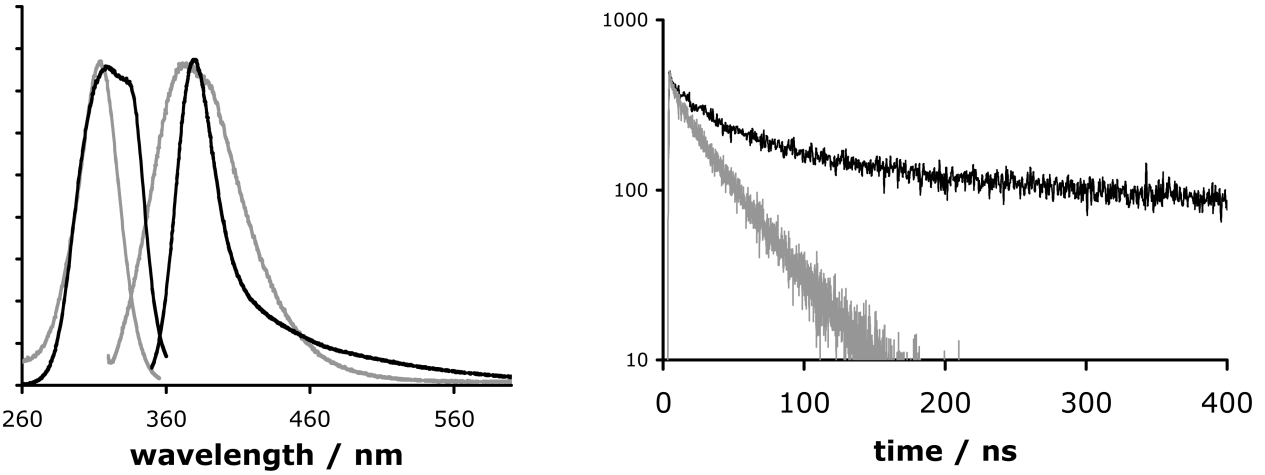

Figure 6. Left: excitation and emission spectra for $[(AuCl)_2(\mu\text{-}\mathbf{3})]$ (gray) and $[Au_2(\mu\text{-}\mathbf{3})_2][PF_6]_2$ (black), in the solid state. Right: decay profiles for $[(AuCl)_2(\mu\text{-}\mathbf{3})]$ (gray) and $[Au_2(\mu\text{-}\mathbf{3})_2][PF_6]_2$ (black).

solid state (Figure 3), with the former conformation placing the two carbenoid rings of the $M(NHC)_2$ unit orthogonal to each other, thus minimizing steric repulsions. In contrast, in the C_2-symmetric conformation the heterocyclic rings are coplanar.

In the ^{13}C NMR spectrum of the silver complex $[Ag_2(\mu\text{-}\mathbf{3})_2][PF_6]_2$ in d_3-acetonitrile a carbene resonance was not observed.[23] However, in d_6-dmso $[Ag_2(\mu\text{-}\mathbf{3})_2][PF_6]_2$ displays a sharp pair of doublets at δ 179.7 ppm for the carbene carbon with coupling constants of 183.5 ($^1J_{^{107}AgC}$) and 212.3 Hz ($^1J_{^{109}AgC}$), respectively. The coupling values are in agreement with a silver bis-carbene species formed rather than a monocarbene complex. As we have previously reported, Ag−C coupling constants in monocarbene complexes are ca. 40−50 Hz greater, in the region of 220 ($J_{^{107}AgC}$) and 260 Hz ($J_{^{109}AgC}$), respectively.[24]

Molar Conductance. Molar conductivity measurements (Λ_M) were carried out for the gold and silver dimers at room temperature within the range of 10^{-3} to 10^{-5} M concentrations, in acetonitrile. The molar conductivity values at 1.0 mM concentrations are 252 and 416 Ω^{-1} cm^2 mol^{-1} for the gold and silver complexes, respectively. The value for $[Au_2(\mu\text{-}\mathbf{3})_2][PF_6]_2$ is within the 220−300 Ω^{-1} cm^2 mol^{-1} range for 2:1 electrolytes;[25] however, that for $[Ag_2(\mu\text{-}\mathbf{3})_2][PF_6]_2$ is well above the upper limit. Comparison between plots of Λ_M vs $c^{1/2}$ (c = molar concentration) allows the determination of the nature of electrolytes, where the same types of electrolytes are expected to have similar slopes. Plots of this nature for the silver and gold complexes $[M_2(\mu\text{-}\mathbf{3})_2][PF_6]_2$ show the molar conductivity decreasing with increasing concentration, as expected due to changes in the interionic forces (Figure S5, Supporting Information). The significant feature of this plot is that the two sets of data have very similar slopes, indicating that both complexes are 2:1 electrolytes.

Electronic Absorption, Luminescence, and Circular Dichroism Spectroscopic Measurements. Luminescence studies undertaken on crystalline samples of the gold complexes $[Au_2(\mu\text{-}\mathbf{3})_2][PF_6]_2$ and $[(AuCl)_2(\mu\text{-}\mathbf{3})]$ showed that they are luminescent in the solid state. In accordance with previous studies into the optical and photophysical behavior of carbene-derived Au(I) complexes, excitation in the UV region was required for observable emission.[14,21] The electronic absorption spectrum of $[Au_2(\mu\text{-}\mathbf{3})_2][PF_6]_2$ in MeCN displays a complex absorption band with a λ_{max} at 245 nm. Although it is red-shifted,

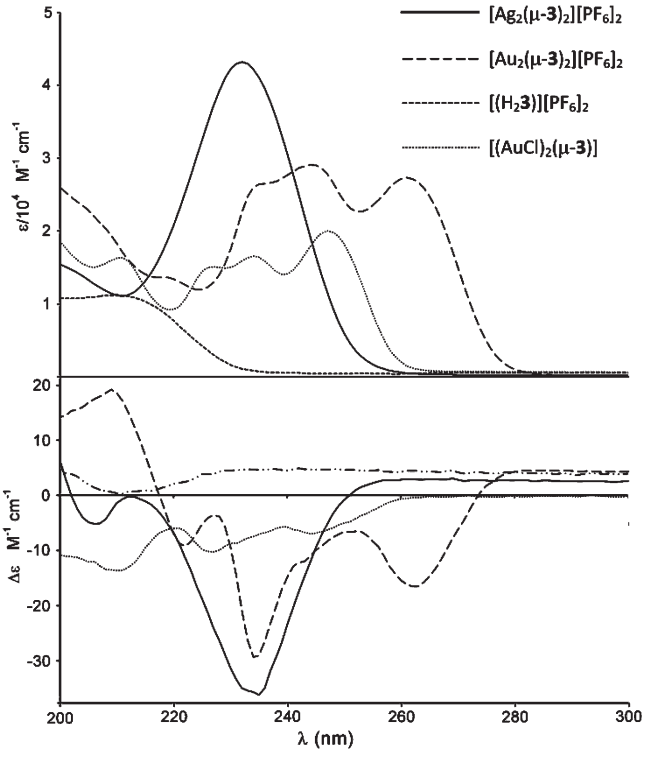

Figure 7. Short-wavelength electronic (top) and circular dichroism (bottom) spectra of $[Ag_2(\mu\text{-}\mathbf{3})_2][PF_6]_2$ (solid curve), $[Au_2(\mu\text{-}\mathbf{3})_2][PF_6]_2$ (long dashes), $[H_2\mathbf{3}][PF_6]_2$ (short dashes), and $[(AuCl)_2(\mu\text{-}\mathbf{3})]$ (dots). Spectra were obtained as approximately equimolar (0.1 mM) acetonitrile solutions at 21 °C.

the main band has an intensity comparable to that of a similar band found in the UV spectrum of the precursor imidazolium salt $[H_2\mathbf{3}][PF_6]_2$. Following excitation at 270−300 nm (Figure 6) $[Au_2(\mu\text{-}\mathbf{3})_2][PF_6]_2$ was found to be emissive at ca. 380 nm. The related complex $[(AuCl)_2(\mu\text{-}\mathbf{3})]$ was similarly emissive, although with a slightly broader emission profile. Complementary time-resolved luminescence studies showed that the complexes exhibited different emission lifetimes. In the solid state, $[(AuCl)_2(\mu\text{-}\mathbf{3})]$ possessed a lifetime (λ_{ex} 295 nm; λ_{em} 380 nm) of 35 ns, whereas

Table 3. X-ray Crystallographic Data

	$[H_23][PF_6]_2$	$[Au_2(\mu\text{-}3)_2][PF_6]_2\cdot H_2O$	$[Ag_2(\mu\text{-}3)_2][PF_6]_2$	$[(AuCl)_2(\mu\text{-}3)]$
empirical formula	$C_{14}H_{20}F_{12}N_4O_2P_2$	$C_{28}H_{38}Au_2F_{12}N_8O_5P_2$	$C_{28}H_{36}Ag_2F_{12}N_8O_4P_2$	$C_{14}H_{18}Au_2Cl_2N_4O_2$
formula wt	566.28	1250.54	1054.33	739.16
cryst syst, space group	monoclinic, $P2_1$	orthorhombic, $I2_12_12_1$	monoclinic, $P2_1$	monoclinic, $P2_1$
a/Å	12.762(2)	13.2240(5)	10.2132(1)	8.3312(3)
b/Å	11.951(2)	17.0310(6)	20.4615(3)	12.6030(4)
c/Å	14.504(2)	20.7230(8)	10.8911(2)	9.4992(4)
α/deg	90	90	90	90
β/deg	99.815(6)	90	106.504(1)	114.071(2)
γ/deg	90	90	90	90
Z	4	4	2	2
no. of data/restraints/params	6163/1/612	4980/0/260	9389/1/509	3742/7/220
final R indices ($F^2 > 2\sigma(F^2)$): R1, wR2	0.0689, 0.1483	0.0561, 0.1257	0.0545, 0.1373	0.0371, 0.0818
R indices (all data): R1, wR2	0.1044, 0.1723	0.0759, 0.1336	0.0583, 0.1403	0.0444, 0.0853

the decay profile of $[Au_2(\mu\text{-}3)_2][PF_6]_2$ fitted well to two contributions: a dominant (86%), long component of 379 ns, and a minor (14%), shorter component (35 ns). The latter contribution is actually attributed to a small amount of $[(AuCl)_2(\mu\text{-}3)]$ in the sample, which was quantitatively identified in solution by ^{1}H NMR spectroscopy.

Gold complexes with short aurophilic contacts can display interesting luminescence properties in the solid state, where the nature of the gold−gold interaction can influence the spectral properties.[3a,b,14,26] However, our observations for the Au−Cl and Au−PF_6 complexes of **3** with the presence or absence of aurophilic interactions as determined by X-ray diffraction (Au−Au distances 3.2948(7) and 6.293(6) Å, respectively) suggest that such interactions do not dominate the emissive character of these complexes. The emission wavelengths of the two gold−**3** complexes are actually comparable to those of the ligand precursor $[H_23][PF_6]_2$, although the peak appearance of the proligand is much broader (Figure S6, Supporting Information) and the emission lifetime of the imidazolium salt is extremely short (0.9 and 4.1 ns with ca. 50/50 weighting) and indicative of fluorescence. Therefore, the wavelength positioning of the observed emission from the complexes probably suggests an excited state which is dominated by ligand-centered character, albeit one significantly perturbed (as indicated by the lifetime decay profiles) by the gold.

In order to measure the effect of the macrocyclic structure on the chiroptical properties of $[Ag_2(\mu\text{-}3)_2][PF_6]_2$ and $[Au_2(\mu\text{-}3)_2][PF_6]_2$, circular dichroism (CD) measurements in the UV region were undertaken. For purposes of comparison, the CD and absorption spectra in the 200−300 nm region of $[Ag_2(\mu\text{-}3)_2][PF_6]_2$, $[Au_2(\mu\text{-}3)_2][PF_6]_2$, $[H_23][PF_6]_2$, and $[(AuCl)_2(\mu\text{-}3)]$ in acetonitrile solution are presented in Figure 7. While no attempt is made here to rigorously assign these spectra, several general observations may be made. The metallamacrocycles $[Ag_2(\mu\text{-}3)_2]^{2+}$ and $[Au_2(\mu\text{-}3)_2]^{2+}$ both display moderately large negative CD values in comparison to the acyclic imidazolium salt $[H_23]^{2+}$. In addition, we observe that while both the CD and absorption spectra of $[Ag_2(\mu\text{-}3)_2]^{2+}$ are relatively simple, the absorption spectra of $[Au_2(\mu\text{-}3)_2]^{2+}$ and $[(AuCl)_2(\mu\text{-}3)]$ are more complex, which is reflected in the complex envelopes of their CD spectra. It is worth noting that, if ligand concentrations are taken into account, the magnitudes of the CD observed for $[Au_2(\mu\text{-}3)_2]^{2+}$ and $[(AuCl)_2(\mu\text{-}3)]$ are roughly comparable, hence implying a small or negligible contribution to the CD derived from the cyclic nature of $[Au_2(\mu\text{-}3)_2]^{2+}$. Given the short wavelengths of these bands, it is not unreasonable to assume that these are largely ligand-centered processes, and we tentatively suggest that the complexity of the Au spectra arises from a larger degree of metal−ligand covalency, resulting in perturbed ligand π levels.[27] This notion is verified to some extent by comparing the bisignate nature of the CD spectrum of $[Au_2(\mu\text{-}3)_2]^{2+}$ at short wavelengths, implying exciton coupling between ligand chromophores within the constraints of the cyclic chiral environment,[28] to the single signed (uncoupled) spectrum of $[(AuCl)_2(\mu\text{-}3)]$.

CONCLUSION

A short synthetic route to the chiral, ether-functionalized NHC precursor $[H_23][PF_6]_2$ has been developed. The bridging ligand **3** forms either cationic dimeric cyclic structures with Ag(I) and Au(I) metals or, in the case of Au(I), neutral bimetallic arrays, depending on the choice of counterion. The neutral and cationic gold complexes are luminescent in the solid state, and lifetime measurements show distinctly different profiles for these two complexes, with the metallamacrocycle $[Au_2(\mu\text{-}3)_2][PF_6]_2$ having an order of magnitude longer emission lifetime (379 ns) in comparison to the acyclic complex $[(AuCl)_2(\mu\text{-}3)]$ (35 ns). The chiral nature of these isomannide-derived compounds has enabled their study by circular dichroism spectroscopy, which, to the best of our knowledge, is the first example of an examination of the chiroptical properties of a carbene complex. Further work is currently in progress on the development of other dehydrohexitol-based NHC derivatives and their applications.

EXPERIMENTAL SECTION

General Remarks. All manipulations were performed using standard glassware under aerobic conditions, except where otherwise noted. Solvents of analytical grade were freshly distilled from sodium/benzophenone (thf, toluene, hexane) or from calcium hydride (CH_2Cl_2, MeCN). DMF (dimethylformamide) was purified by a Braun-SPS solvent purification system. Anhydrous DMA (dimethylacetamide) was purchased from Sigma-Aldrich and used as received. Deuterated solvents for NMR measurements were distilled from the appropriate drying agents under N_2 immediately prior to use, following standard literature methods.[29] All other reagents were used as received. Au(tht)Cl was prepared following a literature procedure.[30] NMR spectra were obtained on Bruker Avance

dx.doi.org/10.1021/om200125w |*Organometallics* 2011, 30, 2553–2562

AMX 400 and 500 and JEOL Eclipse 300 spectrometers. The chemical shifts are given as dimensionless δ values and are frequency referenced relative to TMS for ^{1}H and ^{13}C. Coupling constants J are given in hertz (Hz) as positive values, regardless of their real individual signs. The multiplicities of the signals are indicated as s, d, and m for singlets, doublets, and multiplets, respectively. The abbreviation br is given for broadened signals. Emission, excitation, and lifetime solid-state spectra were acquired on a Jobin Yvon-Horiba Fluorolog spectrometer fitted with a JY TBX picosecond photodetection module. CD spectra were obtained using an Applied Photophysics Chirascan spectrometer equipped with a Xe arc source and a thermostated (21 °C) sample holder. In all cases five spectra were accumulated and averaged. Spectra were measured in the region 200−600 nm at a concentration of approximately 5×10^{-4} M in 0.1 mm quartz cuvettes (Helma). Mass spectra and high-resolution mass spectra were obtained on a Waters LCT Premier XE instrument and are reported as m/z (relative intensity).

Syntheses. *1,4:3,6-2.5-di-O-(p-tolylsulfonyl)-D-mannitol (**2**).* A modified literature procedure was used for the synthesis of **2**.[31] To a solution of 8.5 g (58.2 mmol) of isomannide in 40 mL of dry pyridine cooled in an ice bath was added *p*-tolylsulfonyl chloride (25.6 g, 135 mmol) portionwise. The slurry that formed was stirred overnight. Ice−water (50 mL) was added to the reaction mixture, and the slurry that formed was extracted with chloroform (120 mL). The collected organic layer was washed with 1.25 N hydrochloric acid (3 × 75 mL) until the water layer remained acidic and then with water and finally dried over $MgSO_4$. The chloroform solution was subsequently filtered and the solvent removed under reduced pressure to leave a thick brown oil (22.1 g). Recrystallization from ethanol afforded **2** as a white powder. Yield: 19.9 g, 75%. ^{1}H NMR (400 MHz, $CDCl_3$): δ 2.41 (s, 6H), 3.65 (dd, 1H, ^2J = 9.6, ^3J = 7.7, *endo*-$H^{1/6}$), 3.83 (dd, 1H, ^2J = 9.6, ^3J = 6.8, *exo*-$H^{1/6}$), 4.40 (m, 2H, $H^{3/4}$), 4.78 (m, 2H, $H^{2/5}$), 7.31 (m, 4H, Ar), 7.75 (m, 4H, Ar).

*[H_2**3**][Ts]$_2$.* A sealed pressure tube containing a solution of 4.5 g (9.9 mmol) of 1,4:3,6-2.5-di-*O*-(*p*-tolylsulfonyl)-D-mannitol (**2**) in 4.7 mL (59.4 mmol) of 1-methylimidazole was heated at 140 °C for 3 days. The reaction was followed by TLC (100% ethyl acetate; R_f for **2** = 0.8) until all the ditosylate **2** had reacted. The thick brown oil obtained was washed several times with diethyl ether, to remove the excess methylimidazole. Upon drying $[H_2\mathbf{3}][Ts]_2$ was obtained as a clear foamy material and was used in subsequent reactions without further purification. Yield: 6.07 g, 99%. ^{1}H NMR (400 MHz, d_6-DMSO): δ 2.31 (s, 3H, PhMe), 3.83 (s, 3H, NMe), 4.23 (m, 2H, $H^{1/6}$), 5.12 (d, 1H, $^3J \approx 0$, $H^{3/4}$), 5.25 (m, 1H, $H^{2/5}$), 7.11 (m, 2H, Ar), 7.49 (m, 2H, Ar), 7.82 (m, 2H, imid-*H*), 9.19 (s, 1H, $C_{NHC}H$). MS (ES, CH_3CN): m/z 447.19 ($M - (C_7H_7SO_3)^+$; $C_{21}H_{27}N_4O_5S$ requires 447.17).

*[H_2**3**][PF_6]$_2$.* To a water solution of $[H_2\mathbf{3}][Ts]_2$ (3.16 g, 5.1 mmol, 0.5 M) heated to 45 °C was added a 30 mL water solution of ammonium hexafluorophosphate (8.0 g, 49.1 mmol). During the reaction an off-white solid precipitated, and the mixture was stirred at 45 °C for 1 h and then left at room temperature to complete precipitation of the product. The solid obtained was filtered and dried under vacuum. Yield: 1.85 g, 64%. ^{1}H NMR (400 MHz, d_6-DMSO): δ 3.85 (s, 3H, CH_3), 4.26 (dd, 1H, ^2J = 11.0, ^3J = 2.4, *exo*-$H^{1/6}$), 4.31 (dd, 1H, ^2J = 11.0, ^3J = 4.7, *endo*-$H^{1/6}$), 5.04 (s, 1H, $H^{3/4}$), 5.25 (m, 1H, $H^{2/5}$), 7.76 (m, 2H, imid-*H*), 9.13 (s, 1H, $C_{NHC}H$). ^{1}H NMR (400 MHz, CD_3CN): δ 3.86 (s, 3H, NCH_3), 4.27 (dd, 1H, ^2J = 11.4, ^3J = 2.4, *exo*-$H^{1/6}$), 4.34 (dd, 1H, ^2J = 11.4, ^3J = 4.9, *endo*-$H^{1/6}$), 5.02 (d, $^3J \approx 0$, 1H, $H^{3/4}$), 5.13 (ddd, ^2J = 4.9, ^3J = 2.4, $^3J \approx 0$, 1H, $H^{2/5}$), 7.42 (m, 2H, imid-*H*), 8.48 (s, 1H, $C_{NHC}H$). ^{13}C NMR (125 MHz, d_6-acetone): δ 36.86 (s, CH_3), 66.21 (s, $C^{2/5}$), 72.86 (s, $C^{1/6}$), 88.15 (s, $C^{3/4}$), 122.39 (s, imid-*C*), 125.37 (s, imid-*C*), 137.01 (s, $C_{NHC}H$). UV−vis (CH_3CN, 0.28 mM): λ_{max}/nm ($\varepsilon/10^3$ M^{-1} cm^{-1}): 212 (7.4). IR (KBr) 839 (s), 1101 (s), 1172 (s), 1585 (m), 2912 (w), 3170 (sh, m), 3425 (br, w). MS (ES, CH_3CN): m/z 421.1229 ($M - PF_6^+$; $C_{14}H_{20}N_4O_2PF_6$ requires 421.1228).

*[Ag_2(μ-**3**)$_2$][PF_6]$_2$.* The imidazolium salt $[H_2\mathbf{3}][PF_6]_2$ (0.220 g, 0.39 mmol), Ag_2O (0.092 g, 0.40 mmol), and NaBr (0.410 g, 4.0 mmol) were added to 40 mL of dichloromethane. The mixture was stirred in the dark for 2 days, until the black color of the silver oxide had dissipated. The reaction was monitored by NMR and deemed complete with the disappearance of $\mathbf{3}\cdot(HPF_6)_2$. The reaction mixture was filtered over Celite, which was then washed with dichloromethane (3 × 20 mL). The filtrate was collected and dried under vacuum to afford the silver complex as a white powder. Recrystallization by diffusion of hexane into a dichloromethane solution afforded the product as needle-shaped crystals. Yield: 0.179 g, 85%. ^{1}H NMR (250 MHz, CD_3CN): δ 3.78 (s, 3H; CH_3), 4.23 (dd, ^2J = 11.0, ^3J = 5.1, 1H; *endo*-$H^{1/6}$), 4.43 (dd, ^2J = 11.0, ^3J = 0.7, 1H; *exo*-$H^{1/6}$), 4.74 (d, 1H, $^3J \approx 0$, $H^{3/4}$), 5.20 (dd, ^3J = 5.1, ^3J = 0.7, 1H; $H^{2/5}$), 7.12 (d, ^3J = 1.8, 1H; imid-*H*), 7.16 (d, ^3J = 1.8, 1H; imid-*H*). ^{13}C NMR (125 MHz, CD_3CN): δ 38.57 (s, CH_3), 66.40 (s, $C^{2/5}$), 72.60 (s, $C^{1/6}$), 88.16 (s, $C^{3/4}$), 120.73 (s, imid-*C*), 122.93 (s, imid-*C*), C_{NHC} signal not observed. ^{1}H NMR (400 MHz, d_6-DMSO): δ 3.90 (s, 3H; CH_3), 4.4 (dd, ^2J = 11.0, ^3J = 5.1, 1H; *endo*-$H^{1/6}$), 4.5 (d, ^2J = 11.0, 1H; *exo*-$H^{1/6}$), 4.9 (d, 1H, $^3J \approx 0$, $H^{3/4}$), 5.40 (d, ^3J = 5.1, 1H; $H^{2/5}$), 7.5 (d, 1H; imid-*H*), 7.5 (d, 1H; imid-*H*). ^{13}C NMR (75 MHz, d_6-DMSO): δ (CH_3 signal obscured by acetone peak) 66.51 (s, $C^{2/5}$), 73.16 (s, $C^{1/6}$), 88.59 (s, $C^{3/4}$), 121.92 (s, imid-*C*), 124.10 (s, imid-*C*), 179.74 (dd, $^1J_{^{107}AgC}$ = 183.5, $^1J_{^{109}AgC}$ = 212.3, C_{NHC}). UV−vis (CH_3CN, 0.47 mM): λ_{max}/nm ($\varepsilon/10^3$ M^{-1} cm^{-1}) 232 (42.8). MS (accurate mass, ES$^+$, CH_3CN): m/z (%) calcd mass for $[C_{28}H_{36}{}^{107}Ag_2F_6N_8O_4P]^+$ 907.0603, measured 907.0643.

*[Au_2(μ-**3**)$_2$][PF_6]$_2$ and [(AuCl)$_2$(μ-**3**)]: Reaction in DMF.* A round-bottom flask containing DMF (3.8 mL) was heated to 70 °C, and subsequently Au(tht)Cl (0.203 g, 0.63 mmol) was added. The clear solution was stirred until the entire gold precursor was dissolved. $[H_2\mathbf{3}][PF_6]_2$ (0.340 g, 0.63 mmol) and NaOAc (0.125 g, 1.5 mmol) were added to the solution and the mixture heated to 110 °C for 30 min. While hot, the solution was filtered over Celite into a flask containing 10 mL of water. The precipitated white solid was filtered and the filtrate washed with cold methanol (2 mL) and ether (3 × 5 mL) and dried under vacuum. This afforded 0.258 g of a 1:2 molar mixture (by ^{1}H NMR) of $[Au(\mu\text{-}\mathbf{3})]_2[PF_6]_2$ (yield ∼31%) and $[(AuCl)_2(\mu\text{-}\mathbf{3})]$ (yield ∼62%). X-ray-quality, colorless crystals of $[Au(\mu\text{-}\mathbf{3})]_2[PF_6]_2$ were obtained after storing a saturated DMF solution of the complex for 3 days in the dark.

*[Au_2(μ-**3**)$_2$][PF_6]$_2$ and [(AuCl)$_2$(μ-**3**)]: Reaction in DMA.* A similar procedure was followed in DMA. Au(tht)Cl (0.189 g, 0.59 mmol) was suspended in DMA (3 mL) and heated to 60 °C until the gold complex was dissolved. $[H_2\mathbf{3}][PF_6]_2$ (0.332 g, 0.59 mmol) and NaOAc (0.107 g, 1.31 mmol) were added to the solution and the mixture heated to 70 °C for a few minutes and then to 50 °C for 2 h. Some decomposition to metallic gold was observed during the reaction. The solution was filtered while hot over Celite, and 30 mL of methanol was added to the filtrate to precipitate the product as a white solid. This afforded 0.125 g of a 1:13.5 molar mixture (by ^{1}H NMR) of $[Au(\mu\text{-}\mathbf{3})]_2[PF_6]_2$ (yield ∼4%) and $[(AuCl)_2(\mu\text{-}\mathbf{3})]$ (yield ∼55%). Needle-shaped colorless crystals of $[(AuCl)_2(\mu\text{-}\mathbf{3})]$ were isolated after slow evaporation of an acetonitrile solution.

*[Au_2(μ-**3**)$_2$][PF_6]$_2$.* ^{1}H NMR (400 MHz, CD_3CN): δ 3.90 (s, 3H; CH_3), 4.44 (dd, ^2J = 10.8, ^3J = 6.0, 1H; *endo*-$H^{1/6}$), 4.55 (dd, ^2J = 10.8, ^3J = 3.3, 1H; *exo*-$H^{1/6}$), 5.07 (d, 1H, $^3J \approx 0$, $H^{3/4}$), 5.18 (ddd, ^3J = 6.0, ^3J = 3.3, $^3J \approx 0$, 1H; $H^{2/5}$), 7.24 (d, ^3J = 1.9, 1H; imid-*H*), 7.28 (d, ^3J = 1.9, 1H; imid-*H*). ^{13}C NMR (125 MHz, CD_3CN): δ 38.19 (s, CH_3), 65.98 (s, $C^{2/5}$), 71.20 (s, $C^{1/6}$), 87.816 (s, $C^{3/4}$), 118.44 (s, CH), 123.52 (s, CH), 183.72 (s, C_{NHC}). ^{13}C NMR (100 MHz, CD_3CN): δ 37.48 (s, CH_3), 66.14 (s, $C^{2/5}$), 71.46 (s, $C^{1/6}$), 87.48 (s, $C^{3/4}$), 118.20 (s, CH), 123.10 (s, CH), C_{NHC} not observed. UV−vis (CH_3CN, 0.42 mM): λ_{max}/nm ($\varepsilon/10^3$ M^{-1} cm^{-1}) 235 (25.9), 245 (28.7), 261 (26.9). MS (accurate mass, ES$^+$, CH_3CN): m/z (%) calcd mass for $[C_{28}H_{36}{}^{197}Au_2F_6N_8O_4P]^+$ 1087.1833, measured 1087.1835.

[(AuCl)$_2$(μ-3)]. ^{1}H NMR (250 MHz, CD_3CN): δ 3.79 (s, 3H; CH_3), 4.23 (dd, ^2J = 10.8, ^3J = 2.7, 1H; *exo*-$H^{1/6}$), 4.35 (dd, $^2J_{HH}$ = 10.8, $^3J_{HH}$ = 5.4, 1H; *endo*-$H^{1/6}$), 4.93 (d, 1H, $^3J \approx 0$, $H^{3/4}$), 5.36 (ddd, ^3J = 5.4, ^3J = 2.7, $^3J \approx 0$, 1H; $H^{2/5}$), 7.24 (d, ^3J = 1.9, 1H; imid-*H*), 7.28 (d, ^3J = 1.9, 1H; imid-*H*). ^{13}C NMR (100 MHz, CD_3CN): δ 37.48 (s, CH_3), 66.14 (s, $C^{2/5}$), 71.46 (s, $C^{1/6}$), 87.48 (s, $C^{3/4}$), 118.20 (s, CH), 123.10 (s, CH), C_{NHC} not observed. UV−vis (CH_3CN, 0.38 mM): λ_{max}/nm ($\varepsilon/10^3$ M^{-1} cm^{-1}) 231 (14.7), 235 (28.6), 248 (19.5). MS (ES^+, CH_3CN/d_6-DMSO): *m*/*z* (%) calculated mass for $[M - Cl]^+$ 703.04, measured 703.05 (80).

X-ray Crystallography. All single-crystal X-ray data were collected at 150 K on a Bruker/Nonius Kappa CCD diffractometer using graphite-monochromated Mo Kα radiation (λ = 0.710 73 Å), equipped with an Oxford Cryostream cooling apparatus. Crystal parameters and details of the data collection, solution, and refinement are presented in Table 3. The data were corrected for Lorentz and polarization effects and for absorption using SORTAV.[32] Structure solution was achieved by direct methods (Sir-92 program system)[33] and refined by full-matrix least squares on F^2 (SHELXL-97)[34] with all non-hydrogen atoms assigned anisotropic displacement parameters. Hydrogen atoms were placed in idealized positions and allowed to ride on their parent atoms. In the final cycles of refinement, a weighting scheme that gave a relatively flat analysis of variance was introduced and refinement continued until convergence was reached. Molecular structures in the figures were drawn with ORTEP 3.0 for Windows (version 1.08)[35] and X-Seed.[36] The $[Ag_2(\mu\text{-}3)_2][PF_6]_2$ and $[Au_2(\mu\text{-}3)_2][PF_6]_2$ structures contained large regions of diffusely scattered electron density indicative of severely disordered solvent, which could not be modeled. The SQUEEZE routine in PLATON[37] was used to remove the contributions of the disordered solvent from diffraction intensities in order to improve the refinement of ordered parts within the structures. SQUEEZE details have been appended to the CIF files. The final *F*(000), calculated density, and MW values reflect known species only. Crystallographic data for all compounds have been deposited with the Cambridge Crystallographic Data Centre as supplementary publications CCDC 750149 for $[H_2\mathbf{3}][PF_6]_2$, 750151 for $[Ag_2(\mu\text{-}3)_2][PF_6]_2$, 750150 for $[Au_2(\mu\text{-}3)_2][PF_6]_2$ and 808468 for $[(AuCl)_2(\mu\text{-}3)]$. Copies of the data can be obtained free of charge on application to the CCDC, 12 Union Road, Cambridge CB2 1EZ, U.K. (fax, (+44) 1223 336033; e-mail, deposit@ccdc.cam.ac.uk).

■ ASSOCIATED CONTENT

Supporting Information. Text and figures giving molecular packing diagrams, a molar conductivity graph, and NMR spectra and CIF files giving X-ray crystallographic data for the compounds $[H_2\mathbf{3}][PF_6]_2$, $[Ag_2(\mu\text{-}3)_2][PF_6]_2$, $[Au_2(\mu\text{-}3)_2][PF_6]_2$, and $[(AuCl)_2(\mu\text{-}3)]$. This material is available free of charge via the Internet at http://pubs.acs.org.

■ AUTHOR INFORMATION

Corresponding Author

*A.D.: e-mail, dervisia@cardiff.ac.uk; tel, + 44 (0)29 20874081; fax, + 44 (0)29 20874030.

■ ACKNOWLEDGMENT

We thank Johnson Matthey plc for the loan of hydrated $KAuCl_4$.

■ REFERENCES

(1) (a) Schmidbaur, H.; Schier, A. *Chem. Soc. Rev.* **2008**, *37* (9), 1931. (b) Yam, V. W. W.; Cheng, E. C. C. *Chem. Soc. Rev.* **2008**, *37*, 1806. (c) Panda, T. K.; Roesky, P. W.; Larsen, P.; Zhang, S.; Wickleder, C. *Inorg. Chem.* **2006**, *45*, 7503. (d) Pyykkö, P. *Angew. Chem., Int. Ed.* **2004**, *43*, 4412. (e) Yam, V. W. W.; Chan, C. L.; Li, C. K.; Wong, K. M. C. *Coord. Chem. Rev.* **2001**, *216*−*217*, 173.

(2) (a) Droge, T; Glorius, F. *Angew. Chem., Int. Ed.* **2010**, *49*, 6940. (b) Díez-González, S.; Marion, N.; Nolan, S. P. *Chem. Rev.* **2009**, *109*, 3612. (c) Hahn, F. E.; Jahnke, M. C. *Angew. Chem., Int. Ed.* **2008**, *47*, 3122. (d) Burling, S.; Mahon, M. F.; Reade, S. P.; Whittlesey, M. K. *Organometallics* **2006**, *25*, 3761. (e) Garrison, J. C.; Youngs, W. J. *Chem. Rev.* **2005**, *105*, 3978. (f) Herrmann, W. A. *Angew. Chem., Int. Ed.* **2002**, *41*, 1290.

(3) (a) Gaillard, S.; Slawin, A. M. Z.; Bonura, A. T.; Stevens, E. D.; Nolan, S. P. *Organometallics* **2010**, *29*, 394. (b) Rios, D.; Olmstead, M. M.; Balch, A. L. *Dalton Trans.* **2008**, 4157. (c) Rios, D.; Pham, D. M.; Fettinger, J. C.; Olmstead, M. M.; Balch, A. L. *Inorg. Chem.* **2008**, *47*, 3442. (d) Ray, L.; Shaikh, M. M.; Ghosh, P. *Inorg. Chem.* **2008**, *47*, 230. (e) Mohamed, A. A.; Rawashdeh-Omary, M. A.; Omary, M. A.; Frackler, J. P., Jr. *Dalton Trans.* **2005**, 2597. (f) Wang, J.-W.; Li, Q.-S.; Xu, F.-B.; Song, H.-B.; Zhang, Z.-Z. *Eur. J. Org. Chem.* **2006**, 1310. (g) Khramov, D. M.; Boydston, A. J.; Bielawski, C. W. *Angew. Chem., Int. Ed.* **2006**, *45*, 6186.

(4) Catalano, V. J.; Malwitz, M. A.; Etogo, A. O. *Inorg. Chem.* **2004**, *43*, 5714.

(5) (a) Powell, A. B.; Bielawski, C. W.; Cowley, A. H. *J. Am. Chem. Soc.* **2009**, *131*, 18232. (b) Catalano, V. J.; Etogo, A. O. *Inorg. Chem.* **2007**, *46*, 5608.

(6) Catalano, V. J.; Malwitz, M. A. *Inorg. Chem.* **2003**, *42*, 5483.

(7) Rit, A; Pape, T; Hahn, F. E. *J. Am. Chem. Soc.* **2010**, *132*, 4572.

(8) (a) Liu, B.; Chen, W.; Jin, S. *Organometallics* **2007**, *26*, 3660. (b) Zhou, Y.; Chen, W. *Organometallics* **2007**, *26*, 2742.

(9) Lin, J. C. Y.; Huang, R. T. W.; Lee, C. S.; Bhattacharyya, A.; Hwang, W. S.; Lin, J. B. *Chem. Rev.* **2009**, 3561.

(10) (a) Tennyson, A. G.; Rosen, E. L.; Collins, M. S.; Lynch, V. M.; Bielawski, C. W. *Inorg. Chem.* **2009**, *48*, 6924. (b) Fernández, E. J.; Laguna, A.; López-de-Luzuriaga, J. M. *Dalton Trans.* **2007**, 1969.

(11) (a) Patil, S.; Claffey, J.; Deally, A.; Hogan, M.; Gleeson, B.; Mendez, L. M. M.; Muller-Bunz, H.; Paradisi, F.; Tacke, M. *Eur. J. Inorg. Chem.* **2010**, 1020. (b) Kascatan-Nebioglu, A.; Panzner, M. J.; Tessier, C. A.; Cannon, C. L.; Youngs, W. J. *Coord. Chem. Rev.* **2007**, *251*, 884. (c) Melaiye, A.; Simons, R. S.; Milsted, A.; Pingitore, F.; Wesdemiotis, C.; Tessier, C. A.; Youngs, W. J. *J. Med. Chem.* **2004**, *47*, 973.(d) Herrmann, W. A.; Kocher, C.; Gossen, L. U.S. Patent 6,025,496, 2000. (e) Andrews, J. M. *J. Antimicrob. Chemother.* **2001**, *48*, 5. (f) Kascatan-Nebioglu, A.; Melaiye, A.; Hindi, K.; Durmus, S.; Panzner, M.; Milsted, A.; Ely, D.; Tessier, C. A.; Hogue, L. A.; Mallett, R. J.; Hovis, C. E.; Coughenour, M.; Crosby, S. D.; Cannon, C. L.; Youngs, W. J. *J. Med. Chem.* **2006**, *49*, 6811. (g) Garrison, J. C.; Tessier, C. A.; Youngs, W. J. *J. Organomet. Chem.* **2005**, *690*, 6008.

(12) (a) Raubenheimer, H. G.; Cronje, S. *Chem. Soc. Rev.* **2008**, *37*, 1998. (b) Barnard, P. J.; Berners-Price, S. J. *Coord. Chem. Rev.* **2007**, *251*, 1889. (c) Ray, S.; Mohan, R.; Singh, J. K.; Samantaray, M. K.; Shaikh, M. M.; Panda, D.; Ghosh, P. *J. Am. Chem. Soc.* **2007**, *129*, 15042. (d) Barnard, P. J.; Wedlock, L. E.; Baker, M. V.; Berners-Price, S. J.; Joyce, D. A.; Skelton, B. W.; Steer, J. H. *Angew. Chem., Int. Ed.* **2006**, *45*, 5966.

(13) (a) Boronat, M.; Corma, A.; González-Arellano, C.; Iglesias, M.; Sánchez, F. *Organometallics* **2010**, *29*, 134. (b) Huynh, H. V.; Yeo, C. H.; Chew, Y. X. *Organometallics* **2010**, *29*, 1479. (c) Sakaguchi, S.; Kawakami, M.; O'Neill, J.; Yoo, K. S.; Jung, K. W. *J. Organomet. Chem.* **2010**, *695*, 195. (d) Jafarpour, L.; Nolan, S. P. *J. Organomet. Chem.* **2001**, *17*, 617. (e) Arduengo, A. J., III; Dias, H. V. R.; Calabrese, J. C.; Davidson, F. *Organometallics* **1993**, *12*, 3405. (f) Guerret, O.; Solé, S.; Gornitzka, H.; Teichert, M.; Trinquier, G.; Bertrand, G. *J. Am. Chem. Soc.* **1997**, *119*, 6668. (g) Wang, H. M. J.; Lin, I. J. B. *Organometallics* **1998**, *17*, 972.

(14) (a) Radloff, C.; Wiegard, J. J.; Hahn, F. E. *Dalton Trans.* **2009**, 9392. (b) dit Dominique, F. J. B.; Gornitzka, H.; Sournia-Saquet, A.; Hemmert, C. *Dalton Trans.* **2009**, 340. (c) Zhang, X.; Gu, S.; Xia, Q.; Chen, W. *J. Organomet. Chem.* **2009**, *694*, 2359. (d) Willans, C. E.; Anderson, K. M.; Paterson, M. J.; Junk, P. C.; Barbour, L. J.; Steed, J. W. *Eur. J. Inorg. Chem.* **2009**, 2835. (e) Samantaray, M. K.; Pang, K.; Shaikh,

M. M.; Ghosh, P. *Inorg. Chem.* **2008**, *47*, 4153. (f) Chiu, P. L.; Chen, C. Y.; Lee, C. C.; Hsieh, M. H.; Chuang, C. H.; Lee, H. M. *Inorg. Chem.* **2006**, *45*, 2520. (g) Catalano, V. J.; Moore, A. L. *Inorg. Chem.* **2005**, *44*, 6558. (h) Barnard, P. J.; Baker, M. V.; Berners-Price, S. J.; Skelton, B. W.; White, A. H. *Dalton Trans.* **2004**, 1038. (i) Wanniarachchi, Y. A.; Khan, M. A.; Slaughter, L. M. *Organometallics* **2004**, *23*, 5881. (j) Melaiye, A.; Sun, Z.; Hindi, K.; Milsted, A.; Ely, D.; Reneker, D. H.; Tessier, C. A.; Youngs, W. J. *J. Am. Chem. Soc.* **2005**, *127*, 2285. (k) Garrison, J. C.; Simons, R. S.; Talley, J. M.; Wesdemiotis, C.; Tessier, C. A.; Youngs, W. J. *Organometallics* **2001**, *20*, 1277. (l) Hahn, F. E.; Radloff, C.; Pape, T.; Hepp, A. *Chem. Eur. J.* **2008**, *14*, 10900.

(15) (a) Carcedo, C.; Dervisi, A.; Fallis, I. A.; Ooi, L.; Malik, K. M. A. *Chem. Commun.* **2004**, 1236. (b) Dervisi, A.; Carcedo, C.; Ooi, L. *Adv. Synth. Catal.* **2006**, *348*, 175.

(16) Sohár, P.; Medgyes, G.; Kuszmann, J. *Org. Magn. Reson.* **1978**, *11*, 357.

(17) (a) Grosshans, P.; Jouaiti, A.; Bulach, V.; Planeix, J.-M.; Hosseini, M. W.; Nicoud, J.-F. *Chem. Commun.* **2003**, 1336. (b) Grosshans, P.; Jouaiti, A.; Bulach, V.; Planeix, J.-M.; Hosseini, M. W.; Nicoud, J.-F. *Cryst. Eng. Commun.* **2003**, *5*, 414.

(18) Elbjeirami, O.; Gonser, M.W. A.; Stewart, B. N.; Bruce, A. E.; Bruce, M. R. M.; Cundari, T. R.; Omary, M. A. *Dalton Trans.* **2009**, 1522.

(19) (a) de Fremont, P.; Scott, N. M.; Stevens, E. D.; Ramnial, T.; Lightbody, O. C.; Macdonald, C. L. B.; Clyburne, J. A. C.; Abernethy, C. D.; Nolan, S. P. *Organometallics* **2005**, *24*, 6301. (b) Ray, L.; Katiyar, V.; Barman, S.; Raihan, M. J.; Nanavati, H.; Shaikh, M. M.; Ghosh, P. *J. Organomet. Chem.* **2007**, *692*, 4259. (c) Ray, L.; Katiyar, V.; Raihan, M. J.; Nanavati, H.; Shaikh, M. M.; Ghosh, P. *Eur. J. Inorg. Chem.* **2006**, 3724.

(20) Tripathi, U. M.; Bauer, A.; Schmidbaur, H. *J. Chem. Soc., Dalton Trans.* **1997**, 2865.

(21) (a) Liao, Y.; Ma, J. *Organometallics* **2008**, *27*, 4636. (b) Catalano, V. J.; Etogo, A. O. *J. Organomet. Chem.* **2005**, *690*, 6041.

(22) Bondi, A. *J. Chem. Phys.* **1964**, *68*, 441.

(23) Wang, H. M. J.; Lin, I. J. B. *Organometallics* **1998**, *17*, 972.

(24) Iglesias, M.; Beetstra, D. J.; Knight, J. C.; Ooi, L.; Stasch, A.; Coles, S.; Male, L.; Hursthouse, M. B.; Cavell, K. J.; Dervisi, A.; Fallis, I. A. *Organometallics* **2008**, *27*, 3279.

(25) (a) Geary, W. J. *Coord. Chem. Rev.* **1971**, *7*, 81. (b) Lin, J. C. Y.; Tang, S. S.; Vasam, C. S.; You, W. C.; Ho, T. W.; Huang, C. H.; Sun, B. J.; Huang, C. Y.; Lee, C. S.; Hwang, W. S.; Chang, A. H. H.; Lin, I. J. B. *Inorg. Chem.* **2008**, *47*, 2543.

(26) White-Morris, R. L.; Olmstead, M. M.; Jiang, F.; Tinti, D. S.; Balch, A. L. *J. Am. Chem. Soc.* **2002**, *124*, 2327.

(27) For related two-coordinate Au systems see: Mullice, L. A.; Thorp-Greenwood, F. L.; Laye, R. H.; Coogan, M. P.; Kariuki, B. M.; Pope, S. J. A.; Pope *Dalton Trans.* **2009**, 6836.

(28) For a good example see: Cai., G.; Bozhkova, N.; Odingo, J.; Berova, N.; Nakanishi, K. *J. Am. Chem. Soc.* **1993**, *115*, 7192.

(29) Perrin, D. D.; Amarego, W. F. A. *Purification of Laboratory Chemicals*; Pergamon: Oxford, U.K., 1988.

(30) Bruce, M. I.; Nicholson, B. K.; Shawkataly, O. B. *Inorg. Synth.* **1989**, *26*, 324.

(31) Bakos, J.; Heil, B.; Markó, L. *J. Organomet. Chem.* **1983**, *253*, 249.

(32) Blessing, R. H. *Acta Crystallogr., Sect. A* **1995**, *A51*, 33.

(33) Altomare, A.; Cascarano, G.; Giacovazzo, C.; Guagliardi, A. *J. Appl. Crystallogr.* **1993**, *26*, 343.

(34) Sheldrick, G. M. *SHELXL-97, Program for the Refinement of Crystal Structures*; University of Göttingen, Göttingen, Germany, 1997.

(35) Farrugia, L. J. *J. Appl. Crystallogr.* **1997**, *30*, 565.

(36) Barbour, L. J. *J. Supramol. Chem.* **2001**, *1*, 189.

(37) Spek, A. L. *PLATON, A Multipurpose Crystallographic Tool*; University of Utrecht, Utrecht, The Netherlands, 2003.